Structural, Photophysical and Chiro-Optical Properties of Lanthanide Complexes with a Bis(benzimidazole)pyridine-Based Chiral Ligand

Gilles Muller,[a,b] Christine L. Maupin,[b] James P. Riehl,[b] Henrik Birkedal,[c,d] Claude Piguet,[e] and Jean-Claude G. Bünzli*[a,b]

The neutral Ln^{III} 1:1 nitrato complexes with the chiral ligand 2,6-bis(1-S-neopentylbenzimidazol-2-yl)pyridine (L^{11}) have been synthesised and their stability constants measured in acetonitrile (log K_1 = 4.0–6.4). The crystal and molecular structure of $[Eu(NO_3)_3(L^{11})(MeCN)]$ shows the typical meridional planar coordination of L^{11} to the metal ion and low symmetry of the coordination polyhedron. The influence of the steric hindrance generated by the substituent at R^2 on the crystal packing and bond lengths is discussed. Photophysical measurements show that ligand L^{11} induces a $^3\pi\pi^\star$-to-Ln energy-transfer process in the Eu^{III} complex, while the Tb^{III} compound is ten times less luminescent. Addition of a second molecule of L^{11} to give $[Ln(ClO_4)_2(L^{11})_2]^+$ leads to a large quenching of the Eu^{III} luminescence (140-fold) due to several factors: a less efficient $^1\pi\pi^\star \rightarrow {}^3\pi\pi^\star$ transfer (ca. fourfold), a smaller intrinsic quantum yield Q^{Eu} (ca. threefold), and a substantially less efficient ligand-to-metal transfer (ca. 12-fold). In the case of the Tb^{III} complex, the decrease in the energy of the triplet state reduces further the Tb^{III} emission through increased back transfer. The specific rotary dispersion of the 1:1 and 1:2 complexes points to the chirality of the complexes arising mainly from the ligand, while the circularly polarized luminescence of these complexes with Eu^{III} and Tb^{III} displays a weak effect, pointing to a small diastereomeric excess in solution. Altogether, this study demonstrates that electronic, thermodynamic and photophysical properties of lanthanide complexes with aromatic terdentate ligands can be tuned by modifying the number and the arrangement of the ligands, as well as their substituents, particularly those in the R^2 and R^3 positions.
(© Wiley-VCH Verlag GmbH & Co. KGaA, 69451 Weinheim, Germany, 2003)

Introduction

Present interest in luminescent lanthanide complexes[1] is primarily motivated by applications in life sciences, mainly for developing chemical sensors[2] or tools for medical diagnosis and therapy.[3,4] In this context, the design and use of enantiopure lanthanide compounds present a special advantage with respect to the chiral recognition of biological substrates.[5,6] Lanthanides are subject to fast ligand- and solvent-exchange reactions so that easy interconversion between optical isomers often occurs. Therefore, the use of ligands leading to kinetically inert complexes, such as those derived from the dota (1,4,7,10-tetraazadodecane N,N',N'',N''',-tetraacetic acid) framework favours the isolation of enantiopure compounds.[7] We have recently reported on the first diastereoselective formation in solution of lanthanide triple helical complexes with a terdentate chiral C_2-symmetric ligand **L(−)** (Scheme 1) derived from terpyridine, as was suggested by their specific rotary dispersion, circularly polarized luminescence (CPL) and NMR spectra.[8] We have also investigated the influence of chiral groups grafted onto aromatic tridentate ligands on the diastereomeric induction in solution. For instance, ligands **L*** and **L12**, with a chiral group in the pyridine 4-position, form thermodynamically stable 1:3 triple helical complexes with Ln^{III} ions in acetonitrile, and chiro-optical measurements suggest the helical wrapping of the ligand strands around the Ln^{III} ions, while the CPL data are in agreement with a small diastereomeric excess in solution.[9,10]

Working along these lines, we have introduced a chiral substituent onto the benzimidazole sidearms of bis(benzimidazole)pyridine to yield **L11**. However, the bulky neopentyl group precludes the formation of stable triple helical com-

[a] Institute of Molecular and Biological Chemistry, Swiss Federal Institute of Technology, BCH 1402,
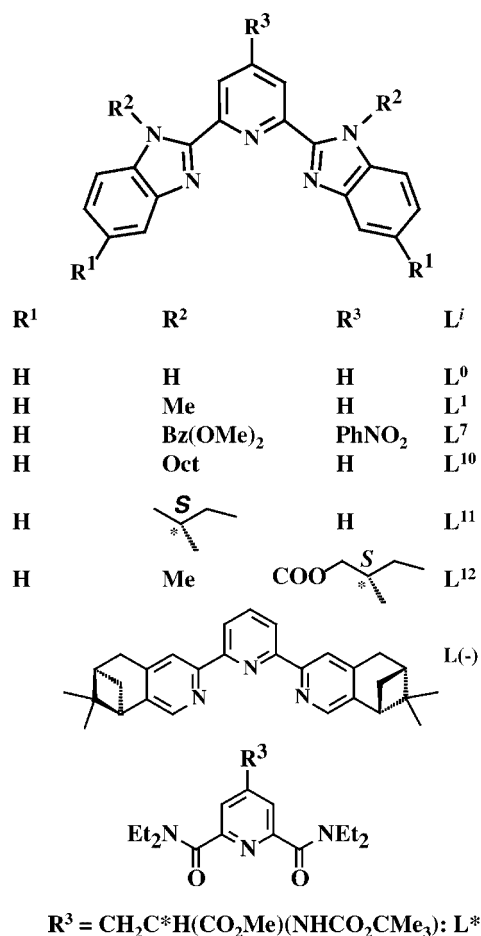CH-1015 Lausanne, Switzerland
E-mail: jean-claude.bunzli@epfl.ch
[b] Department of Chemistry, University of Minnesota Duluth, Duluth, MN, 55812-3020, USA
[c] Institute of Crystallography, BSP, University of Lausanne, CH-1015 Lausanne, Switzerland
[d] Department of Chemistry and Biochemistry, University of California,
Santa Barbara, CA 93106, USA
[e] Department of Inorganic, Analytical and Applied Chemistry, University of Geneva,
30 quai E. Ansermet, CH-1211 Geneva 4, Switzerland
  Supporting information for this article is available on the WWW under http://www.eurjic.org or from the author.

R^1	R^2	R^3	L^i
H	H	H	L^0
H	Me	H	L^1
H	Bz(OMe)$_2$	PhNO$_2$	L^7
H	Oct	H	L^{10}
H	S (sec-butyl)	H	L^{11}
H	Me	COO–(sec-butyl)	L^{12}

$R^3 = CH_2C^*H(CO_2Me)(NHCO_2CMe_3): L^*$

Scheme 1

plexes: in the X-ray structure of [Eu(L^{11})$_3$](ClO$_4$)$_3$·4.28MeCN, two of the ligand molecules are wrapped around the Eu^{III} ion in a helical fashion, much as they are in the 1:2 complex with La^{III}, while the third one lies more or less perpendicular to the other two.[11] To further our understanding of the influence of helical wrapping on diastereomeric induction, we investigate here the thermodynamic, structural, luminescent and chiro-optical properties of the neutral nitrato complexes [Ln(NO$_3$)$_3$(L^{11})] (Ln = La, Eu, Tb) and compare them to those of [Ln(ClO$_4$)$_2$(L^{11})$_2$]$^+$ complexes in solution.

Results and Discussion

Isolation, Structure and Stability of the 1:1 Nitrato Complexes

Neutral 1:1 complexes form easily upon mixing equivalent amounts of hydrated lanthanide nitrate and L^{11} in dichloromethane/acetonitrile. The general formula of the isolated complexes is [Ln(NO$_3$)$_3$(L^{11})(MeCN)$_x$] [x = 0, La (**1**), Gd (**3**), Tb (**4**); x = 1, Eu (**2**)] where the acetonitrile molecule sometimes completes the inner-sphere of the Ln^{III} ion to a coordination number of 10 (see below), but can be removed by heating under vacuum. Complexation is evi-

denced in the IR spectra by the blue shift of the two C=C benzimidazole and pyridine vibrational modes by 2−5 and 11−14 cm^{-1}, respectively (Table S1). Nitrate ions behave as bidentate ligands with local C_{2v} symmetry as exemplified by energy differences $\Delta(\nu_1 - \nu_4)$ larger than 180 cm^{-1}:[12] 221, 228, 229, and 230 cm^{-1} for La, Eu, Gd, and Tb, respectively. Single crystals suitable for X-ray diffraction analysis were obtained for the Eu complex **2**. The atom-numbering scheme is displayed in Figure 1 and selected bond lengths and angles are reported in Table 1, while interplanar angles are listed in Table S2. The structure consists of neutral molecules with 10-coordinate Eu^{III}, the metal ion being bound to six O atoms from the three bidentate nitrate anions, one N atom from the solvating molecule and three N atoms from L^{11}. The ligand is coordinated in the usual meridional planar way, as was observed for [Eu(NO$_3$)$_3$(L^1)(MeOH)],[13] with two small and very similar interplanar angles between the pyridine and benzimidazole moieties, α_{pb} = 6.5° and 6.2°, as compared to 3.3° and 5.5° for L^{11}, but in contrast to the situation found in [Eu(NO$_3$)$_3$(L^7)(MeCN)]·2.5MeCN[14] and [Eu(NO$_3$)$_3$(L^{10})].[13] Indeed, in the former, L^7 is bent with two different angles
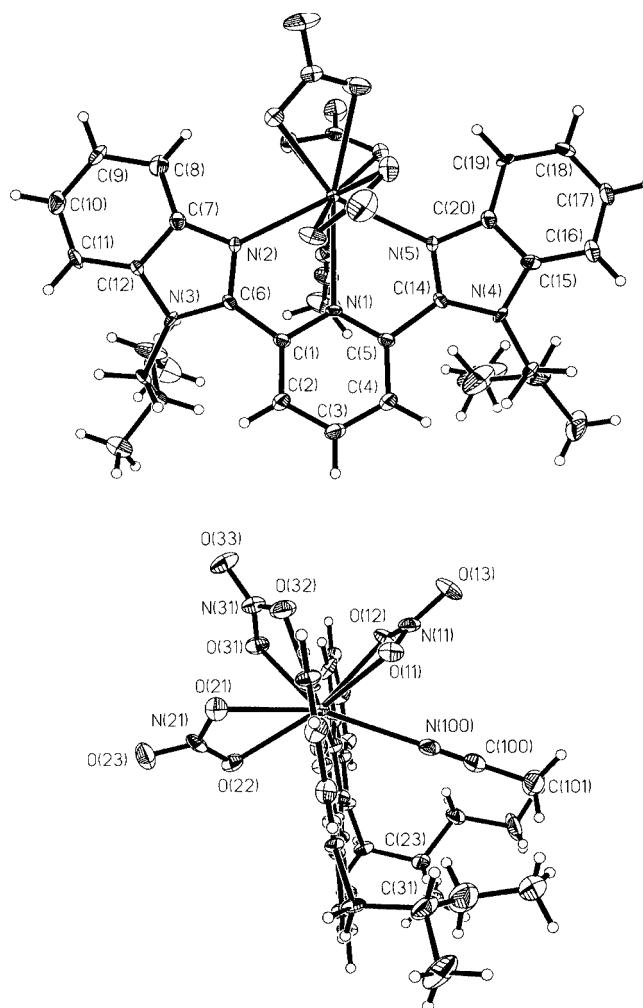

Figure 1. Two views of the molecular structure of [Eu(NO$_3$)$_3$(L^{11})(MeCN)] showing the atom-numbering scheme

Table 1. Bond lengths (Å) and angles (deg) in the coordination polyhedron of [Eu(NO$_3$)$_3$(**L^{11}**)(MeCN)]

Bond lengths

Eu1−N1	2.627(4)	Eu1−N100	2.735(5)	Eu1−O21	2.592(5)
Eu1−N2	2.470(7)	Eu1−O11	2.486(7)	Eu1−O22	2.535(5)
Eu1−N5	2.470(7)	Eu1−O12	2.478(7)	Eu1−O31	2.492(5)
				Eu1−O32	2.562(6)

Bond angles

N1−Eu1−N2	63.8(3)	N5−Eu1−O21	70.8(2)	O21−Eu1−N100	151.7(2)
N1−Eu1−N5	63.1(3)	N5−Eu1−O22	88.8(2)	O22−Eu1−O31	71.9(2)
N2−Eu1−N5	126.9(1)	N5−Eu1−O31	139.1(2)	O22−Eu1−O32	104.7(2)
N1−Eu1−O11	117.8(2)	N5−Eu1−O32	103.9(2)	O22−Eu1−N100	127.1(2)
N1−Eu1−O12	124.8(2)	N5−Eu1−N100	81.2(3)	O31−Eu1−O32	50.7(2)
N1−Eu1−O21	99.6(2)	O11−Eu1−O12	52.1(2)	O31−Eu1−N100	139.2(2)
N1−Eu1−O22	66.6(2)	O11−Eu1−O21	112.2(2)	O32−Eu1−N100	128.2(1)
N1−Eu1−O31	132.1(2)	O11−Eu1−O22	161.5(2)	N1−Eu1−N11	125.2(1)
N1−Eu1−O32	163.5(2)	O11−Eu1−O31	109.2(2)	N2−Eu1−N11	104.9(3)
N1−Eu1−N100	62.6(1)	O11−Eu1−O32	66.0(2)	N5−Eu1−N11	103.6(3)
N2−Eu1−O11	126.4(2)	O11−Eu1−N100	64.7(2)	N100−Eu1−N11	162.9(1)
N2−Eu1−O12	82.0(2)	O12−Eu1−O21	135.5(2)	N31−Eu1−N11	79.9(2)
N2−Eu1−O21	120.3(2)	O12−Eu1−O22	142.3(2)	N1−Eu1−N31	153.9(2)
N2−Eu1−O22	72.0(2)	O12−Eu1−O31	77.9(2)	N2−Eu1−N31	105.9(2)
N2−Eu1−O31	81.8(2)	O12−Eu1−O32	70.9(2)	N5−Eu1−N31	122.7(2)
N2−Eu1−O32	128.5(2)	O12−Eu1−N100	67.0(2)	N100−Eu1−N31	140.4(1)
N2−Eu1−N100	73.5(3)	O21−Eu1−O22	50.1(2)	O11−Eu1−N11	25.8(3)
N5−Eu1−O11	78.6(2)	O21−Eu1−O31	69.1(2)	O21−Eu1−N11	127.4(2)
N5−Eu1−O12	128.8(2)	O21−Eu1−O32	65.3(2)	O31−Eu1−N11	94.0(2)

α_{pb} = 4.3° and 13.1°, while in the latter the two benzimidazole arms of **L^{10}** are not coplanar with the central pyridine (α_{pb} = 29.7° and 28.3°). The observation of different conformations for these ligands may be explained by the crystal packing and the steric hindrance generated by the R^2 groups. In [Eu(NO$_3$)$_3$(**L^{11}**)(MeCN)], the crystal packing is governed by several weak intermolecular CH···O H-bonds, involving the O-atoms of the nitrate anion N2 (Figure 2 and Table S3). Each coordinated O atom generates one interaction with H atoms located on the neopentyl arms or on the phenyl groups of another complex molecule, while the non-coordinated O-atom is involved in similar interactions with H atoms from acetonitrile or from the neopentyl groups of a different complex molecule. The steric hindrance of the
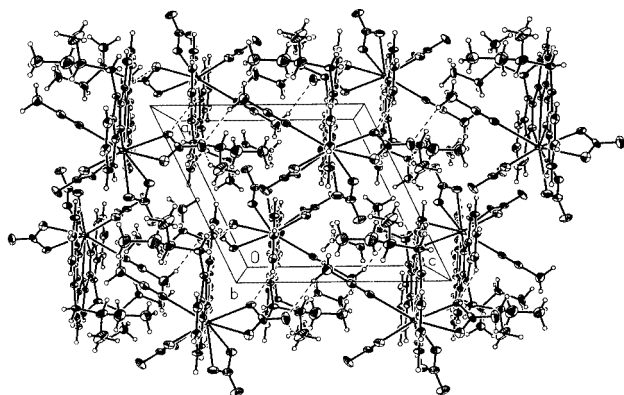

Figure 2. Intermolecular CH···O interactions observed in the crystal structure of [Eu(NO$_3$)$_3$(**L^{11}**)(MeCN)]

neopentyl groups increases the bend of the ligand slightly, as previously observed for [Eu(NO$_3$)$_3$(**L^{10}**)], so that the interstrand π-stacking interactions evidenced in [Eu(NO$_3$)$_3$-(**L^1**)(MeOH)] are lost.[13] Furthermore, the asymmetric conformation of the two benzimidazole units in [Eu(NO$_3$)$_3$(**L^7**)(MeCN)]·2.5MeCN can be explained by the presence of strong intermolecular interactions, induced by the bulky dimethoxybenzyl substituents, with nitrate anions.[14]

The coordination environment of the Eu^{III} ion in **2** is best described as a distorted 4:5:1 polyhedron (Figure S1) similar to the arrangement observed in the complexes with **L^1** [13] and **L^7**.[14] In comparison with [Eu(NO$_3$)$_3$(**L^1**)(MeOH)], the complexes with **L^7** and **L^{11}** feature an acetonitrile molecule coordinated to the Eu^{III} ion instead of a methanol molecule. This difference does not influence the characteristics of the coordination polyhedron. However, the Eu−N(MeCN) distance in **2** (2.735 Å) is substantially longer than those found in the complex with **L^7** (2.555 Å)[14] and in the solvate [Sm(MeCN)$_9$]$^{3+}$ (2.54 Å).[15] This lengthening is a consequence of the acetonitrile molecule in **2** being implied in an intermolecular interaction with a nitrate anion (see above). The capping position of the polyhedron is occupied by N2 from one of the benzimidazole units, while the two planes are defined by O11, O21 and O31 from the three nitrate anions and N5 from the second benzimidazole substituent, and O12, O22 and O32 from the nitrates, N1 from the central pyridine, and N100 from the coordinated acetonitrile molecule. The two Eu−N(benzimidazole) bonds are symmetric (Table 1), in contrast to the situation

with L^1, L^7 and L^{10} where the two Eu–N(benzimidazole) distances are different, but in all cases shorter than the Eu–N(pyridine) bond. On the other hand, we note that the mean Eu–N distances in the complexes with L^{10} and L^{11} are similar (2.52 Å) and shorter than in the complexes with ligands bearing small R^2 groups such as hydrogen {2.58 Å, [Eu(NO$_3$)$_2$(L^0)$_2$](NO$_3$)[16]} or methyl (2.54 Å, L^1).[13] Generally speaking, this mean value decreases with the increase of the steric hindrance generated by the R^2 substituents. However, the mean Eu–N distance of 2.57 Å in the complex with L^7, which contains the bulky dimethoxybenzyl groups, is quite close to the value determined for the complex with L^0, a consequence of the influence of the electron-attracting *p*-nitrophenyl group substituted in the R^3 position of the central pyridine ring.

All three bidentate nitrate anions bound to the metal ion in **2** have an approximate C_{2v} local symmetry and present Eu–O bonds in the range 2.48–2.59 Å, with an average distance of 2.52 Å, similar to the values observed in related nitrato complexes (2.46–2.55 Å).[13,14,16] The ionic radius calculated according to Shannon's definition (1.17 Å) is the same as in the other 10-coordinate complexes (1.16–1.17 Å)[13,14,16] and is close to the expected value of 1.18 Å.[17] Finally, it should be mentioned that the two asymmetric carbon atoms, C21 and C23, retain their absolute configuration *S* in the complex, as was observed in the free ligand.[11]

In order to gain information on the stability of the 1:1 nitrato complexes, we performed spectrophotometric and luminescence titrations of L^{11} with Ln(NO$_3$)$_3$ (Ln = La, Eu, Tb, Lu) at 298 K in MeCN, in the presence of 0.1 M Et$_4$NClO$_4$, under N$_2$ atmosphere. Factor analysis[18] indicates the presence of two absorbing species and the fit converges for log K_1 = 4.0 ± 0.4, 4.0 ± 0.5, 4.0 ± 0.5, and 6.4 ± 0.2 for La, Eu, Tb, and Lu, respectively. For La, the stability constant is similar to the value determined for L^1 (4.2 ± 0.3).[19] The log K_1 value of the Eu^{III} complex determined by luminescence titration is in good agreement with that extracted from the spectrophotometric data: 4.1 ± 0.4.

Luminescent Properties of the Nitrato 1:1 and Perchlorato 1:2 Complexes in Solution

The electronic spectrum of L^{11} in MeCN displays one intense band centred at 31385 cm^{-1}, which splits into two components upon complexation, reflecting the electronic transformations associated with the *trans-trans → cis-cis* conformational change and the complexation of the Ln^{III} metal to the tridentate binding unit (Table 2).[13,20] UV irradiation of L^{11} at room temperature yields one broad unresolved fluorescence band, centred around 27100 cm^{-1}, and originating from the $^1\pi\pi^*$ state (Figure 3). Upon complexation to non-luminescent Ln^{III} ions, the energy of the ligand $^1\pi\pi^*$ state decreases by about 2000 and 2770 cm^{-1} in the 1:1 and 1:2 complexes, respectively. At 77 K, the ligand triplet state appears at 21120 cm^{-1} and undergoes a bathochromic shift of 90–185 cm^{-1} in the nitrato complexes and of 755 cm^{-1} in the La^{III} 1:2 perchlorato complex (Table 2); lifetimes decrease from 389 ± 4 ms for the free

ligand to 215 ± 1 and 93 ± 5 ms for the La 1:1 and 1:2 complexes, respectively. In addition to the weak metal-centred emission bands, the luminescence spectra of the Eu^{III} and Tb^{III} solutions reveal emission from the ligand $^1\pi\pi^*$ state. The latter is more intense in the case of the 1:2 complexes (see Figure 3), for which the ratio between the integrated ligand-centred singlet state and metal-centred emission bands reaches a factor of 280, compared to about one in the nitrato complexes. The mechanism by which energy is transferred from the ligand to the metal ion involves two essential steps, an intersystem crossing (isc) from the singlet to the triplet state of the ligand and energy transfer to the long-lived excited $^5D_0$(Eu) or $^5D_4$(Tb) states.[1] To get a better insight into the various energy migration processes occurring in the 1:1 and 1:2 complexes, we determined the quantum yield of both the ligand- and metal-centred luminescence of 10^{-4} to 10^{-3} M solutions at 293 K upon ligand excitation, and the ratio between the integrated triplet and singlet state emissions, $R_{TS} = I^T/I^S$, for the free ligand and its La (or Gd) complexes at 77 K.

The fluorescence quantum yield of the free ligand, Q^F = 78%, is smaller than for L^1, for which it is close to 100%. It is substantially reduced by factors of 55 (La) and 83 (Gd) in the 1:1 nitrato complexes, but only by a factor of nine in the perchlorato 1:2 complex with La. Simultaneously, the ligand-centred phosphorescence is enhanced upon complexation as shown by R_{TS} which increases from 1.5×10^{-4} for uncomplexed L^{11} to 5.5×10^{-3} (La) and 1.5×10^{-2} (Gd) in the nitrato complexes, and to 1.5×10^{-3} in the La 1:2 complex. The better isc efficiency in 1:1 complexes results (i) from a more favourable energy gap between the $^1\pi\pi^*$ and $^3\pi\pi^*$ states: $\Delta E(^3\pi\pi^* - ^1\pi\pi^*)$ = 4640 (La) and 4450 (Gd) cm^{-1}, as compared to 6660 cm^{-1} in the free ligand and to 5690 cm^{-1} in its 1:2 complex with La (ideal value of 5000 cm^{-1}, Figure 4),[21] and (ii) from the mixing of the ligand-centred singlet and triplet wavefunctions promoted by spin-orbit and/or paramagnetic effects.[22]

The overall quantum yield of the europium-centred luminescence obtained upon ligand excitation, Q_L^{Eu}, amounts to 1.4% for the nitrato 1:1 complex, as compared to 2.8% for the corresponding compound with L^1.[19] This quantum yield can be broken down according to the following equation:

$$Q_{tot}^{Eu} = \eta_{ISC} \cdot \eta_{ET} \cdot Q^{Eu} = \eta_{sens} \cdot Q^{Eu}$$

where Q^{Eu} is the intrinsic luminescence quantum yield of the Eu^{III} ion, η_{sens} the efficiency of the luminescence sensitisation by the ligand, and η_{ISC} and η_{ET} the yields of the intersystem crossing and of the ligand-to-metal energy transfer, respectively. The intrinsic quantum yield Q^{Eu} is simply the ratio between the observed and radiative lifetimes of the Eu($^5D_0$) level:

$$Q^{Eu} = \tau_{obs}/\tau_R$$

In turn, in the special case of Eu^{III}, for which the intensity of the magnetic dipole $^5D_0 \rightarrow ^7F_1$ transition is in prin-

Table 2. Ligand-centred absorptions in acetonitrile, ligand-centred singlet- and triplet-state energies as determined from emission spectra of solutions 10^{-3} M in MeCN for the ligand L^{11} and its 1:1 and 1:2 complexes

Compound	$E(x\rightarrow\pi^*)$/cm^{-1} 293 K	$E(^1\pi\pi^*)$/cm^{-1} 293 K	77 K[c]	$E(^3\pi\pi^*)$/cm^{-1} 77 K [c]
L^{11}	31385 (4.48)			21120
			27780	19685
		27100	26810	18780
[La(NO$_3$)$_3$(L^{11})]	31950 (4.44)			*20935*
	30120 (4.44)	27250 sh	25575	19640
		25250	24750	18360
[Eu(NO$_3$)$_3$(L^{11})(MeCN)]	32465 (4.41)	26845	[d]	[e]
	28925 (4.46)	25445		
[Gd(NO$_3$)$_3$(L^{11})]	32260 (4.41)			21030
	28820 (4.46)	27360 sh	25480	19630
		25000	24600	18315
[Tb(NO$_3$)$_3$(L^{11})]	32465 (4.44)		[d]	[e]
	28820 (4.44)	24785		
[La(ClO$_4$)$_2$(L^{11})$_2$]$^+$	32050 (4.69)		26055	
	29585 (4.71)		24845	20365
		24330	23895	18330
[Eu(ClO$_4$)$_2$(L^{11})$_2$]$^+$	32585 (4.60)	26845 sh	[d]	[e]
	28530 (4.57)	23875		
[Tb(ClO$_4$)$_2$(L^{11})$_2$]$^+$	32580 (4.69)		[d]	[e]

[a] sh = shoulder; at the concentration used, about 97, and 72−77% of the metal ion is under the form of the 1:2 and 1:1 complexes and 3, and 23−28% under the form of the 1:1 complex and free ligand in 1:2 and 1:1 solutions, respectively. [b] x = n or π; Logε values are given between parentheses. [c] The 0-phonon transition is given in italics for frozen solutions in MeCN. [d] Not measured. [e] Not observed because of the $L11$-to-Ln energy transfer process.
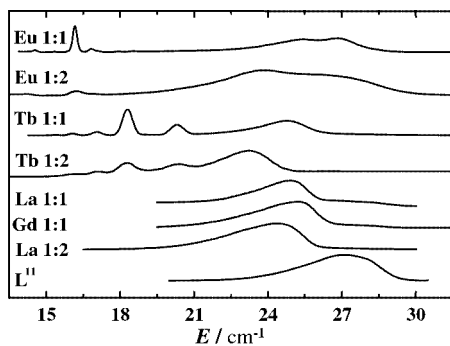

Figure 3. Emission spectra of [Ln(NO$_3$)$_3$(L^{11})(MeCN)$_x$] (x = 0, 1), [Ln(ClO$_4$)$_2$(L^{11})$_2$]$^+$, and L^{11} 10^{-3} M in MeCN at 293 K

ciple independent of the chemical environment, the radiative lifetime τ_R can be estimated from:[23]

$$\tau_R = [1/(A_{MD,0}\cdot n^3)]\cdot(I_{MD}/I_{tot})$$

in which $A_{MD,0}$ is the spontaneous emission probability of the Eu($^5D_0\rightarrow{}^7F_1$) transition (14.65 s^{-1}), n is the refractive index (1.34 for the acetonitrile solution) and I_{MD}/I_{tot} is the intensity ratio of the Eu($^5D_0\rightarrow{}^7F_1$) transition to the total emission of the $^5D_0$ level. For the 1:1 complex, I_{MD}/I_{tot} = 0.1, leading to τ_R = 2.8 ms, Q^{Eu} = 0.47 (τ_{obs} = 1.32 ± 0.01 ms) and η_{sens} = 0.03. The isc efficiency in [La(NO$_3$)$_3$$L^{11}$] is about three times larger than in the nitrato La complex with L^1. Since the energy gaps $\Delta E(^3\pi\pi^*-{}^5D_0)$ are comparable — ca. 3600 cm^{-1} and 3700 cm^{-1} for the complexes with L^1 and L^{11}, respectively, as estimated from $E(^3\pi\pi^*)$ in the La complexes — the smaller overall quantum
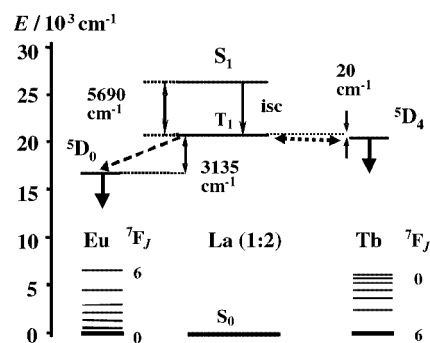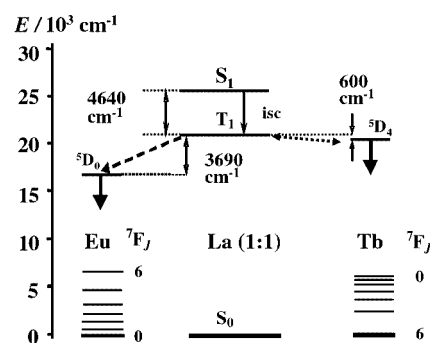

Figure 4. Schematic energy diagram for [Ln(NO$_3$)$_3$(L^{11})(MeCN)$_x$] (x = 0, 1) and [Ln(ClO$_4$)$_2$(L^{11})$_2$]$^+$ complexes; data for S_1 and T_1 are those of the La^{III} complexes in frozen solution at 77 K (0-phonon transitions)

yield of $[Eu(NO_3)_3L^{11}]$ compared with the L^1 complex can be traced back to more efficient non-radiative deactivation processes taking place in the former complex, probably in view of the larger fluxionality induced by the neopentyl substituents.

The situation is different in the Eu 1:2 complexes with L^{11} for which the quantum yield drops to 1×10^{-2} %. With respect to the nitrato 1:1 complex, the $\Delta(^3\pi\pi^* - ^5D_0)$ gap decreases from ca. 3700 cm^{-1} to ca. 3100 cm^{-1}, which should be more favourable for the sensitisation of the metal luminescence. On the other hand, the isc process is about four times less efficient (compare the R_{TS} values given above for the La complexes) and the intrinsic quantum yield is smaller: a calculation similar to the one above leads to $I_{MD}/I_{tot} = 0.18$, $\tau_R = 5.1$ ms, $Q^{Eu} = 0.14$ ($\tau_{obs} = 0.73 \pm 0.01$ ms). Consequently, $\eta_{sens} = 7 \times 10^{-4}$, that is 42-fold smaller than in the 1:1 complex. Therefore, the 140-fold drop in the overall quantum yield of the 1:2 complex compared with the 1:1 compound can be roughly broken into three contributions: a less-efficient $^1\pi\pi^* \rightarrow ^3\pi\pi^*$ transfer (ca. fourfold), a smaller intrinsic quantum yield Q^{Eu} (ca. threefold), and a substantially less efficient ligand-to-metal transfer (ca. 12-fold). A similar, but much more dramatic decrease in the overall quantum yield (3400-fold) has been reported for $[Eu(L^1)_3]^{3+}$ compared with $[Eu(NO_3)_3(L^1)(MeOH)]$. This effect was assigned, both on the basis of experimental data[19] and theoretical modelling,[24] to the presence of a ligand-to-metal charge transfer (LMCT) state with an energy close to that of the ligand singlet state.

The Tb^{III} complexes are about ten times less luminescent than the Eu^{III} analogues, with $Q_L^{Tb} = 1.1 \times 10^{-1}$ and 1.3 $\times 10^{-3}$ % for the 1:1 and 1:2 complexes, respectively. The main reason is a deactivation through energy back-transfer onto the ligand since the energy gap $\Delta(^3\pi\pi^* - ^5D_4)$ amounts to only 600 and 20 cm^{-1}, respectively. The more efficient back-transfer taking place in the 1:2 complex compared with the nitrato compound is exemplified by the temperature dependence of the $^5D_4(Tb)$ lifetimes, which are longer, for solid state samples, than for the nitrato complex.[25]

Chiro-Optical Properties

The specific rotary dispersion of solutions of the $[Ln(NO_3)_3(L^{11})(MeCN)_x]$ ($x = 0, 1$) complexes (10^{-3} M in anhydrous acetonitrile) amounts to 18.8 ± 0.8 (La), 17.1 ± 0.2 (Eu), 16.8 ± 0.3 (Gd) and 19.1 ± 0.3 (Tb) deg·dm^2·mol^{-1}. These values are close to the one measured for the free ligand (15.1 ± 0.3 deg dm^2 mol^{-1}), pointing essentially to no structural contribution to the chiro-optical effect. For the 1:2 complexes, a similarly small structural contribution (4−5 deg dm^2 mol^{-1}) has been evidenced.[11] As a comparison, 4- to 10-fold larger rotary dispersion values have been observed for 1:3 complexes with ligands L^{12}[10] and L^*[9] compared with the free ligand value, pointing to the importance of the structural contribution in triple-stranded chiral helical complexes.

We have resorted to circularly polarized luminescence (CPL) to determine whether or not the 1:3 complex with

L^{11} presents an enantiomeric excess of one isomer. CPL spectra were measured for solutions of $[Eu(NO_3)_3(L^{11})$-$(MeCN)]$, $[Ln(ClO_4)_2(L^{11})_2]^+$ (Ln = Eu, Tb) $1−1.6 \times 10^{-3}$ M and for a perchlorate solution containing an Eu:L^{11} ratio equal to 1:34. In the latter, high resolution luminescence spectra (in a mixture of anhydrous MeCN:CH$_2$Cl$_2$, 97:3) show that the 1:3 species exists in a proportion of about 20% (Figure S2), the remaining Eu-containing species being the 1:2 complex, while only 1% of the Eu^{III} ions are in the 1:3 form in a 10^{-3} M perchlorate solution with a stoichiometric 1:3 ratio. The excitation spectrum of $[Eu(ClO_4)_2(L^{11})_2]^+$ 10^{-3} M in the range of the $^5D_0 \leftarrow ^7F_0$ transition reveals the presence of two bands at 17260 and 17244 cm^{-1} originating from the 1:1 and 1:2 complexes, respectively (Figure S3). The presence of the 1:1 species in the 10^{-3} M $[Eu(ClO_4)_2(L^{11})_2]^+$ solution is confirmed by the speciation that can be calculated from the stability constants:[11] a 10^{-3} M solution contains 97% of the 1:2 species and about 3% of the 1:1 species. However, the quantum yield of the latter is 140 times larger than for the 1:2 compound, which explains the observation of both species in the excitation spectrum with similar intensity.

The emission of the magnetic dipolar $^5D_0 \rightarrow ^7F_1$ transition is circularly polarized for the three Eu^{III} solutions with very small ΔI values, the smallest effect occurring, as expected, for the 1:1 species (Figure 5). We interpret these data as follows. The CPL properties observed for $[Eu(NO_3)_3(L^{11})$-$(MeCN)]$ result solely from the effect of the chirality of the ligand, while for the 1:2 and 1:3 compounds, the structural contribution of the helical wrapping of the ligands also contributes to ΔI. It is noteworthy that for the solutions of the perchlorato complexes, ΔI depends on the polarisation of the excitation light, indicating the presence of more than a single species in solution.[26] The CPL spectrum of the corresponding terbium 1:2 perchlorato complex displays a low ΔI value (Figure S4), which also demonstrates that the compound is not a racemic mixture in solution. Therefore, the chiro-optical data presented here are consistent with the presence of small diastereomeric excesses in solutions of the 1:2 and 1:3 complexes, on the short time scale of optical
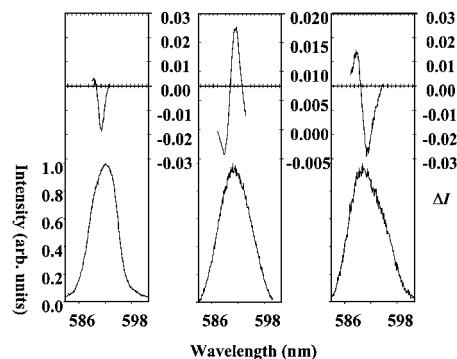

Figure 5. CPL spectrum of the $^5D_0 \rightarrow ^7F_1$ transition of $1−1.6 \times 10^{-3}$ M solutions of $[Eu(NO_3)_3(L^{11})(MeCN)]$ (left), $[Eu(ClO_4)_2$-$(L^{11})_2]^+$ (middle) in anhydrous MeCN and one with an Eu:L^{11} ratio of 1:34 (right) in a mixture of anhydrous MeCN and CH$_2$Cl$_2$ (97:3) at 293 K

measurements, as previously observed for 1:3 complexes with L^{12} [10] and $L*$.[9]

Conclusion

The structural properties of $[Eu(NO_3)_3(L^{11})(MeCN)]$ are similar to those of the Eu^{III} complexes with ligands L^1 and L^7. Upon complexation, the ligand adopts a *cis-cis* configuration which implies a meridional planar coordination of the Eu^{III} metal. The introduction of various substituents in the R^2 position influences both the inner coordination sphere of the metal ion and the crystal packing, which is mainly governed by intermolecular interactions involving hydrogen bonds. The addition of a second ligand in the perchlorato 1:2 complexes significantly modifies the photophysical properties. For Eu^{III}, an efficient quenching of the metal-centred luminescence occurs which is due to several factors, one of which could be lowering of the energy of the LMCT state. Ligand L^{11} is not a good sensitizer of the Tb^{III} luminescence in view of its too low-lying triplet state, and the introduction of a second ligand molecule lowers the energy of this state still further, leading to increased energy back-transfer. This study confirms that electronic, thermodynamic and photophysical properties of lanthanide complexes with aromatic terdentate ligands can be tuned by modifying the number, the arrangement and the nature of the ligands. In particular, the nature of electron-attracting or -withdrawing R^2 or R^3 groups influences critically the physicochemical properties of the complexes. Contrary to what was observed for the tris complexes with L^{12},[10] $L*$ [9] and $L(-)$,[8] the chiro-optical properties of the 1:2 and 1:3 complexes mainly arise from the chirality of the ligand and not from a structural contribution due to the helical wrapping of the ligand strands around the Ln^{III} ions. On the other hand, small enantiomeric excesses are generated in solutions of 1:2 and 1:3 complexes.

Experimental Section

Solvents and Starting Materials: Acetonitrile and dichloromethane were distilled from CaH_2. Other products were purchased from Fluka AG (Buchs, Switzerland) or Merck and used without further purification. The ligand L^{11}, its 1:2 complexes and lanthanide perchlorates and nitrates were synthesised as described previously.[11,27]

Caution: Dry perchlorates and their complexes with aromatic amines may easily explode and should be handled in small quantities and with extreme precaution.[28]

Spectroscopic and Analytical Measurements: Electronic spectra in the UV/Vis range were recorded at 293 K with a Perkin−Elmer Lambda 900 spectrometer using 1.0 and 0.1 cm quartz cells. Specific rotary dispersion values were measured from 10^{-3} M solutions in degassed anhydrous acetonitrile at 298 K with the help of a JASCO DIP-370 polarimeter (sodium D line). IR spectra were obtained from KBr pellets with a Mattson α-Centauri FT-IR spectrometer. Ligand excitation and emission spectra were recorded on a Perkin−Elmer LS-50B spectrometer equipped for low temperature (77 K) measurements. The experimental procedures for high resolution, laser excited luminescence studies have been published

previously.[29] Emission spectra are corrected for the instrument function. Quantum yields of the ligand-centred emission were measured relative to quinine sulfate in 0.05 M H_2SO_4 ($A_{347} = 0.05$, absolute quantum yield: 0.546).[30] Quantum yields of the metal-centred emission were determined as described previously[19] at excitation wavelengths at which (i) the Lambert−Beer law is obeyed, and (ii) the absorption of the reference $[Ln(terpy)_3]^{3+}$ closely matches that of the sample. CPL measurements were made on an instrument described previously, operating in a differential photon-counting mode.[26] Elemental analyses were performed by Dr H. Eder (Microchemical Laboratory, University of Geneva).

Spectrophotometric Titrations: The electronic spectra in the UV/Visible range were recorded at 298 K from 10^{-4} M solutions in acetonitrile containing Et_4NClO_4 0.1 M as inert electrolyte with a Perkin−Elmer Lambda 7 spectrometer connected to an external personal computer and using quartz cells of 0.100 cm path length. Solutions were prepared in a thermostatted vessel (Metrohm 6.1418.220) and the titrating solution was added with an automated burette from Metrohm (6.1569.150 or -.210) fitted with an anti-diffusion device. In a typical experiment, 5−10 cm³ of L^{11} were titrated with a solution of Ln^{III} nitrate 10^{-4} M in acetonitrile, under N_2 atmosphere. After each addition of 0.10 cm³ and a delay of 2 min, the spectrum was measured and transferred to the computer. Factor analysis and stability constant determinations were carried out with the program SPECFIT, version 2.10 ($\pm 2\sigma$).[31]

Crystal Structure of $[Eu(NO_3)_3(L^{11})(MeCN)]$: The block-shaped crystals were directly transferred from the mother liquor into a drop of Hostinert 216 and kept at 210 K. A specimen was selected and placed in a glass capillary. The data collection took place at 150 K on a Stoe IPDS system equipped with Mo-K_α radiation. The detector-crystal distance was set to 80 mm, and a φ interval of 1° was chosen. Two hundred images were collected with an exposure time of 10 min/image. The integration was based on an effective mosaic spread of 0.011 and a profile of between 9 and 21 pixels. The intensities were corrected for Lorentz and polarisation effects. No absorption correction could be applied since the crystal was all but invisible in the frozen oil, but the absorption coefficient appears to be small. The decay during the measurement was negligible. The structure was solved and refined on F^2 with the help of the SHELX system.[32] In the final model, a part of the ligand was described with isotropic atomic displacement parameters and all atoms in L^{11} were submitted to rigid link restraints. All hydrogen atoms were clearly visible in the difference electron density maps, and were included in a riding atom model. The last cycles continued to show a non-zero maximal parameter chance over σ. This is due to the fact that the Flack parameter[33] (refined as a component in the least-squares) turns negative at the end of each of the final cycles; it is then reset to zero by the program. The structure was analysed using SHELXTL 5.05[34] and PLATON.[35] The refinement favours the S configuration for the chirality centres C21 and C23, as expected from the synthesis.

Crystal Data: $C_{31}H_{36}EuN_9O_9$, $M = 830.65$, monoclinic, space group $P2_1$ (N_0 4), $a = 10.172(2)$, $b = 16.804(3)$, $c = 10.989(2)$ Å, $U = 1697.2(6)$ Å³, $T = 150(2)$ K, $Z = 2$, $\mu(Mo-K_\alpha) = 1.915$ mm⁻¹, 10740 reflections measured, 5205 unique ($R_{int} = 0.1013$) which were used in all calculations. The final $wR(F^2)$ was 0.0347 (all data). CCDC-217485 contains the supplementary crystallographic data for this paper. These data can be obtained free of charge at www.ccdc.cam.ac.uk/conts/retrieving.html [or from the Cambridge Crystallographic Data Centre, 12, Union Road, Cambridge CB2 1EZ, UK; Fax: (internat.) + 44-1223/336-033; E-mail: deposit@ccdc.cam.ac.uk].

Preparation of the 1:1 Nitrato Complexes: The 1:1 complexes $[Ln(NO_3)_3(\mathbf{L^{11}})(MeCN)_x]$ [$x = 0$, La (**1**), Gd (**3**), Tb (**4**); $x = 1$, Eu (**2**)] were prepared by mixing equivalent amounts of $Ln(NO_3)_3 \cdot nH_2O$ (Ln = La, Eu, Gd, Tb and $n = 5-6$) and $\mathbf{L^{11}}$ in dichloromethane/acetonitrile (1:4 v/v) and the residual suspension was refluxed for 30 min. The complexes were crystallised in $70-80\%$ yield by slow evaporation of the solvent and were characterised by their IR spectra (Table S1) and elemental analyses. [$C_{29}H_{33}LaN_8O_9$ (776.53): calcd. C 44.9, H 4.3, N 14.4; found C 44.9, H 4.3, N 14.3. $C_{31}H_{36}EuN_9O_9$ (830.64): calcd. C 44.8, H 4.4, N 15.2; found C 44.6, H 4.3, N 15.0. $C_{29}H_{33}GdN_8O_9$ (794.88): calcd. C 43.8, H 4.2, N 14.1; found C 43.9, H 4.3, N 14.1. $C_{29}H_{33}N_8O_9Tb$ (796.55): calcd. C 43.7, H 4.2, N 14.1; found C 43.7, H 4.1, N 14.1].

Acknowledgments

[1] J.-C. G. Bünzli, *Spectroscopic Properties of Rare Earths in Optical Materials* (Eds.: G. K. Liu and B. Jacquier), Springer Verlag, Berlin, **2003**, Ch. 11, in press.

[2] D. Parker, *Coord. Chem. Rev.* **2000**, *205*, 109−130.

[3] J.-C. G. Bünzli, in *Metal Ions in Biological Systems* (Eds.: A. Sigel and H. Sigel), Marcel Dekker Inc., New York, **2003**, Vol. 42, Ch. 2, in press.

[4] V. W. W. Yam, K. K. W. Lo, *Coord. Chem. Rev.* **1998**, *184*, 157−240.

[5] G. Bobba, R. S. Dickins, S. D. Kean, C. E. Mathieu, D. Parker, R. D. Peacock, G. Siligardi, M. J. Smith, J. A. G. Williams, C. F. G. C. Geraldes, *J. Chem. Soc., Perkin Trans. 2* **2001**, 1729−1737.

[6] H. Tsukube, S. Shinoda, *Chem. Rev.* **2002**, *102*, 2389−2403.

[7] D. Parker, R. S. Dickins, H. Puschmann, C. Crossland, J. A. K. Howard, *Chem. Rev.* **2002**, *102*, 1977−2010.

[8] G. Muller, J.-C. G. Bünzli, J. P. Riehl, D. Suhr, A. von Zelewsky, H.-R. Mürner, *Chem. Commun.* **2002**, 1522−1523.

[9] G. Muller, B. Schmidt, J. Jiricek, G. Hopfgartner, J. P. Riehl, J.-C. G. Bünzli, C. Piguet, *J. Chem. Soc., Dalton Trans.* **2001**, 2655−2662.

[10] G. Muller, J. P. Riehl, K. J. Schenk, G. Hopfgartner, C. Piguet, J.-C. G. Bünzli, *Eur. J. Inorg. Chem.* **2002**, 3101−3110.

[11] G. Muller, J.-C. G. Bünzli, K. J. Schenk, C. Piguet, G. Hopfgartner, *Inorg. Chem.* **2001**, *40*, 2642−2651.

[12] K. Nakamoto, *Infrared and Raman Spectra of Inorganic and Coordination Compounds. Part A. Theory and Applications in Inorganic Chemistry*, Wiley Interscience, New York, **1997**.

[13] C. Piguet, A. F. Williams, G. Bernardinelli, E. Moret, J.-C. G. Bünzli, *Helv. Chim. Acta* **1992**, *75*, 1697−1717.

[14] S. Petoud, J.-C. G. Bünzli, K. J. Schenk, C. Piguet, *Inorg. Chem.* **1997**, *36*, 1345−1353.

[15] H. Jingyu, S. Qi, J. Zhongsheng, *Kexue Tongbao (Chin. Sci. Bull.)* **1990**, *35*, 1090−1092.

[16] W. Shuangxi, Z. Ying, C. Yuxin, W. Liufang, L. Qinhui, *J. Chem. Soc., Dalton Trans.* **1994**, 2523−2530.

[17] R. D. Shannon, *Acta Crystallogr., Sect. A* **1976**, *32*, 751−767.

[18] E. R. Malinowski and D. G. Howery, *Factor Analysis in Chemistry*, John Wiley, New York, Chichester, Brisbane, Toronto, **1980**.

[19] S. Petoud, J.-C. G. Bünzli, T. Glanzman, C. Piguet, Q. Xiang, R. P. Thummel, *J. Lumin.* **1999**, *82*, 69−79.

[20] C. Piguet, J.-C. G. Bünzli, G. Bernardinelli, C. G. Bochet, P. Froidevaux, *J. Chem. Soc., Dalton Trans.* **1995**, 83−97.

[21] F. J. Steemers, W. Verboom, D. N. Reinhoudt, E. B. van der Tol, J. W. Verhoeven, *J. Am. Chem. Soc.* **1995**, *117*, 9408−9414.

[22] S. Tobita, M. Arakawa, I. Tanaka, *J. Phys. Chem.* **1984**, *88*, 2697−2702. S. Tobita, M. Arakawa, I. Tanaka, *J. Phys. Chem.* **1985**, *89*, 5649−5654.

[23] M. H. V. Wertz, R. T. F. Jukes, J. W. Verhoeven, *Phys. Chem. Chem. Phys.* **2002**, *4*, 1542−1548.

[24] F. R. Gonçalves e Silva, R. Longo, O. L. Malta, C. Piguet, J.-C. G. Bünzli, *Phys. Chem. Chem. Phys.* **2000**, *2*, 5400−5403.

[25] G. Muller, PhD. Dissertation, University of Lausanne, **2000**.

[26] J. P. Riehl, F. S. Richardson, *Chem. Rev.* **1986**, *86*, 1−16.

[27] J.-C. G. Bünzli, J.-R. Yersin, C. Mabillard, *Inorg. Chem.* **1982**, *21*, 1471−1476.

[28] W. C. Wolsey, *J. Chem. Educ.* **1973**, *50*, A335−A337.

[29] R. Rodríguez-Cortiñas, F. Avecilla, C. Platas-Iglesias, D. Imbert, J.-C. G. Bünzli, A. de Blas, T. Rodríguez-Blas, *Inorg. Chem.* **2002**, *41*, 5336−5349.

[30] S. R. Meech, D. C. Phillips, *J. Photochem.* **1983**, *23*, 193−217.

[31] H. Gampp, M. Maeder, C. J. Meyer, A. D. Zuberbühler, *Talanta* **1985**, *23*, 1133−1139.

[32] G. M. Sheldrick, *Acta Crystallogr., Sect. A* **1997**, *46*, 467−473.

[33] H. D. Flack, *Acta Crystallogr., Sect. A* **1983**, *39*, 876−881.

[34] G. M. Sheldrick, SHELXTL 5.05 Siemens Analytical X-ray Instruments Inc., Madison, WI, **1996**.

[35] A. L. Spek, *Acta Crystallogr., Sect. A* **1990**, *46*, C34.